Neuron, Volume *58*

Supplemental Data

A Precisely Timed Asynchronous Pattern of ON and OFF Retinal Ganglion Cell Activity during Propagation of Retinal Waves

Supplemental Experimental Procedures

All experiments were carried out according to the guidelines of the Institutional Animal Care and Use Committee at the University of Washington and in compliance with the National Institutes of Health *Guide for the Care and Use of Laboratory Animals*.

Recordings

In experiments without pharmacological interventions, spontaneous activity was first recorded in complete darkness for > 1hr followed by visual stimulation. Alternatively, spontaneous activity was recorded in complete darkness in control conditions and in the presence of the respective pharmacological agents for > 1 hr each, with full-field stimuli presented at the beginning and end of the recording. We routinely subdivided both segments of spontaneous activity and analyzed several parts separately to control the stability of the recording and to avoid mistaking continuous changes in the structure of waves during the course of an experiment for pharmacological effects. On numerous occasions washout was permitted leading in all cases to recovery of waves of similar structure to those preceding the pharmacological intervention.

Data Analysis

BPI

We use the BPI to assess the preference of cells to burst together (BPI >) or apart (BPI < 0). It is worth mentioning that cells with perfectly synchronized activity could still have a *BPI = 0* if their activity were strictly periodic such that $R_{xy}(-1) = R_{xy}(0) = R_{xy}(1)$. As illustrated in Figure S1 the bursting of RGCs, however, was not periodic in the vast majority of cases (36 of 39 retinas). In the few retinas (3 of 39) that showed oscillatory burst patterns the delay between bursts of a given cell was ~2 s such that peaks in the cross-correlogram at 1 s or -1s were restricted to opposite sign cell pairs. We use the BPI solely as a tool to compress the correlation structure of the activity of cell pairs in order to allow for easier demonstration of pharmacological effects on activity patterns in 2D plots.

Identification of Bursts and Waves

Several patterns are evident in the firing of spontaneously active RGCs at the ages recorded (P10 – P15). Spikes of a single unit tended to occur in short bursts of high frequency discharge. The presence of simultaneous or adjacent bursts of several units in a recording field and the spread of this activity between recording fields indicated the propagation of retinal waves. In addition, single units often fired several closely spaced bursts during a wave. We used the following algorithms to automatically identify bursts and waves in our multielectrode data. First, in each spike train potential bursts were designated based on a minimum number of spikes (4) and a maximum interval between them (0.4 s). The statistical significance of each burst was then evaluated using a modified Poisson surprise method (Legendy and Salcman, 1985). This computed the probability (P_C) of observing the same number of spikes (C) as observed in the current burst, in a Poisson spike train of the same mean firing rate (r) in a segment equal to the duration of the current burst (T) according to:

$$P_C = \frac{e^{-rT} \times (rT)^C}{C!} \quad (1)$$

When the probability that a Poisson spike train would generate the same number of spikes as observed was < 10^{-4}, the respective burst was accepted. Wave identification proceeded by a similar algorithm. First, potential waves were identified in each burst train based on a maximum interval between bursts (5 s). Bursts separated by less than this interval were fused together. However, as no minimum for the number of bursts per wave was defined, also single bursts passed this step and were designated possible waves. This was necessary as the number of bursts per wave varied with age and particularly at P10 waves often consisted of single bursts. The significance of each potential wave was then assessed by counting the number of spikes (C) from other units in the same recording field during the respective time interval of length T and determining the probability (P_C) that Poisson spike trains of equivalent mean firing rate (r) would generate the same number of spikes according Equation (1). As above when $P_C < 10^{-4}$ waves were accepted. The identification of bursts was controlled by comparing the average width of bursts defined by our algorithm with that estimated from the full-width at half-maximum of the spike train autocorrelograms (Demas et al., 2003) of a random subset of cells. Differences between these measures were statistically insignificant ($p > 0.1$). In addition, for each recording we made sure that our algorithm identified > 90% of the bursts and waves identified by eye on a segment of the recording.

Supplemental References

Brandstatter, J.H., Koulen, P., Kuhn, R., van der Putten, H., and Wassle, H. (1996). Compartmental localization of a metabotropic glutamate receptor (mGluR7): two different active sites at a retinal synapse. J. Neurosci. *16*, 4749–4756.

Brivanlou, I.H., Warland, D.K., and Meister, M. (1998). Mechanisms of concerted firing among retinal ganglion cells. Neuron *20*, 527–539.

Butts, D.A., Kanold, P.O., and Shatz, C.J. (2007). A burst-based "Hebbian" learning rule at retinogeniculate synapses links retinal waves to activity-dependent refinement. PLoS Biol. *5*, e61. 10.1371/journal.pbio.0050061.

Demas, J., Eglen, S.J., and Wong, R.O. (2003). Developmental loss of synchronous spontaneous activity in the mouse retina is independent of visual experience. J. Neurosci. *23*, 2851–2860.

Diao, L., Sun, W., Deng, Q., and He, S. (2004). Development of the mouse retina: emerging morphological diversity of the ganglion cells. J. Neurobiol. *61*, 236–249.

Koulen, P., and Brandstatter, J.H. (2002). Pre- and postsynaptic sites of action of mGluR8a in the mammalian retina. Invest. Ophthalmol. Vis. Sci. *43*, 1933–1940.

Lee, C.W., Eglen, S.J., and Wong, R.O. (2002). Segregation of ON and OFF retinogeniculate connectivity directed by patterned spontaneous activity. J. Neurophysiol. *88*, 2311–2321.

Legendy, C.R., and Salcman, M. (1985). Bursts and recurrences of bursts in the spike trains of spontaneously active striate cortex neurons. J. Neurophysiol. *53*, 926–939.

Pan, F., Mills, S.L., and Massey, S.C. (2007). Screening of gap junction antagonists on dye coupling in the rabbit retina. Vis. Neurosci. *24*, 609–618.

		$ON_{Control}$	ON_{Drug}	p	n (n ret.)	$OFF_{Control}$	OFF_{Drug}	p	n (n ret.)
L-APB (50μM)	Firing rate (Hz)	0.33 ± 0.03	0.7 ± 0.06	p<0.001	46(6)	0.55 ± 0.09	1.11 ± 0.1	p<0.001	46(6)
	Burst duration (s)	0.48 ± 0.02	0.59 ± 0.04	p<0.03		0.67 ± 0.07	0.78 ± 0.09	p>0.05	
	Interwave interval (s)	110 ± 19	34 ± 8	p<0.001		47 ± 6.9	16 ± 2.2	p<0.001	
Carbenoxolone (50μM)	Firing rate (Hz)	0.59± 0.17	0.61 ± 0.06	p>0.2	20(3)	0.77 ± 0.15	0.79 ± 0.25	p>0.9	24(3)
	Burst duration (s)	0.64 ± 0.04	0.58 ± 0.05	p>0.9		0.73 ± 0.08	0.63 ± 0.06	p>0.4	
	Interwave interval (s)	66 ± 27	59 ± 7.6	p>0.2		35 ± 6.7	55 ± 20	p>0.9	
Meclofenamic acid (200μM)	Firing rate (Hz)	0.24 ± 0.04	0.34 ± 0.1	p>0.5	20(2)	0.54 ± 0.08	0.53 ± 0.08	p>0.5	22(2)
	Burst duration (s)	0.51 ± 0.04	0.68 ± 0.18	p>0.8		0.62 ± 0.06	0.54 ± 0.05	p>0.05	
	Interwave interval (s)	206 ± 21	116 ± 22	p<0.003		69 ± 14	59 ± 12	p<0.02	
TPMPA (50μM)	Firing rate (Hz)	0.38± 0.05	0.71 ± 0.09	p<0.01	19(3)	0.59 ± 0.23	0.90 ± 0.30	p<0.01	18(3)
	Burst duration (s)	0.58 ± 0.08	0.60 ± 0.08	p>0.2		0.65 ± 0.13	0.58 ± 0.14	p>0.2	
	Interwave interval (s)	108 ± 20	61 ± 5.0	p<0.01		75 ± 21	48 ± 11	p<0.01	
Gabazine (5μM)	Firing rate (Hz)	0.44± 0.15	2.3 ± 0.33	p<0.001	18(3)	0.52 ± 0.10	2.5 ± 0.31	p<0.001	16(3)
	Burst duration (s)	0.55 ± 0.03	0.61 ± 0.05	p>0.4		0.73 ± 0.12	0.91 ± 0.23	p>0.9	
	Interwave interval (s)	201 ± 37	30 ± 2.7	p<0.02		63 ± 14	23 ± 1.9	p<0.01	
Strychnine (500 nM)	Firing rate (Hz)	0.53± 0.08	3.1 ± 0.25	p<0.001	33 (6)	1.2 ± 0.18	1.6 ± 0.17	p>0.1	32(6)
	Burst duration (s)	0.42 ± 0.02	0.50 ± 0.02	p<0.01		0.78 ± 0.07	0.98 ± 0.15	p<0.001	
	Interwave interval (s)	96 ± 19	8.7 ± 0.34	p<0.001		37 ± 7.6	16 ± 1.2	p>0.2	
Strychnine (500 nM), Gabazine (5μM), TPMPA (50μM)	Firing rate (Hz)	0.34± 0.03	4.2 ± 0.70	p<0.001	26 (5)	0.57 ± 0.04	1.9 ± 0.23	p<0.001	29(5)
	Burst duration (s)	0.55 ± 0.07	0.46 ± 0.04	p<0.001		0.58 ± 0.09	0.30 ± 0.05	p<0.001	
	Interwave interval (s)	180 ± 27	14 ± 1.2	p<0.001		93 ± 15	17 ± 1.5	p<0.001	

Table S1. Pharmacological Effects on Spontaneous Activity of ON and OFF RGCs at P12
Average firing rates, burst durations and interwave intervals for spontaneous activity of ON and OFF RGCs in the absence or presence of the indicated pharmacological agents are shown. Entries in all cases are mean ± SEM. Statistical significance of changes in the firing of RGCs was assessed using a Wilcoxon signed rank test. Importantly, burst duration was relatively stable to pharmacological intervention allowing us to use the same index of burst preference in all cases.

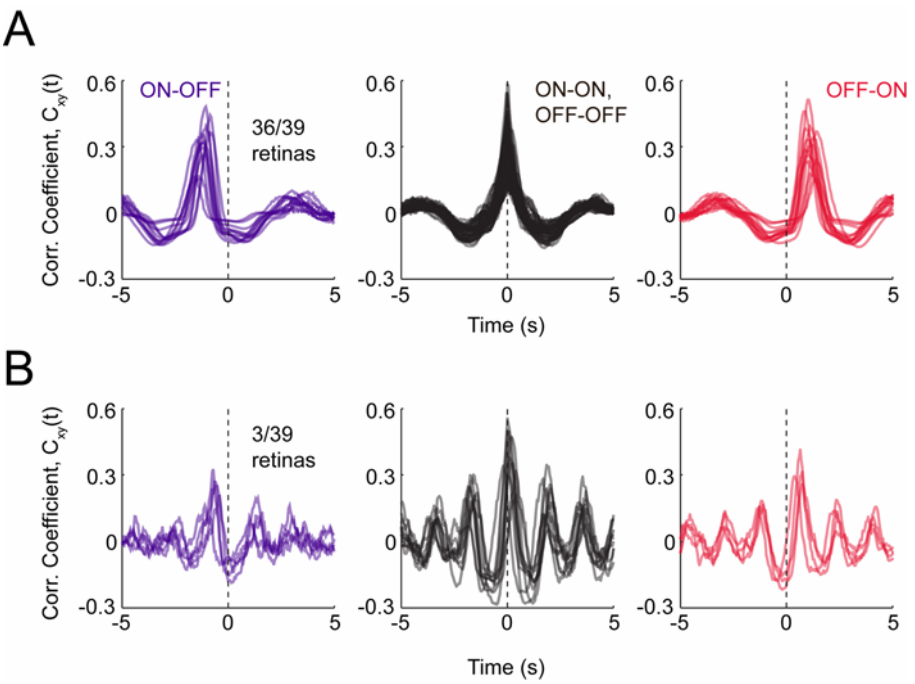

Figure S1. Repetitive Bursts of ON and OFF RGCs during Glutamatergic Waves Are Not, in the Majority of Cases, Oscillatory

(A and B) Cross-correlations for all combinations of spike trains of spontaneously active RGCs within one electrode field recorded in representative experiments at P12 are shown. (A) Repetitive bursts during waves in > 90% of the retinas recorded (36 of 39) were not oscillatory as indicated by the single high peak in the cross-correlogram between -5 and 5s. An interesting feature in the cross-correlograms of same sign cell pairs are the negative going troughs on either side of the central peak. This means that same sign cells which tend to burst together are less likely than expected by chance to burst adjacently. In light of burst based plasticity rules that predict weakening of connections that fire adjacent bursts (Butts et al., 2007), silence during this period might serve to avoid weakening of connections that are meant to be strengthened. (B) In a small fraction of the retinas (3 of 39) recorded, bursting of RGCs was more rhythmic as indicated by multiple peaks in the cross-correlation function. Even in these cases, however, cross-correlograms of opposite sign cell pairs were asymmetric showing a higher peak for the bursting of OFF cells after ON cells. Together, these observations argue that the activity pattern of ON and OFF RGCs during glutamatergic waves is not explained by two (ON and OFF) phase shifted oscillators, but that instead the activity of OFF RGCs is locked to that of ON RGCs in precisely-timed fashion. The interval from an OFF burst to the next ON burst and the interval between bursts of each cell were in most cases variable.

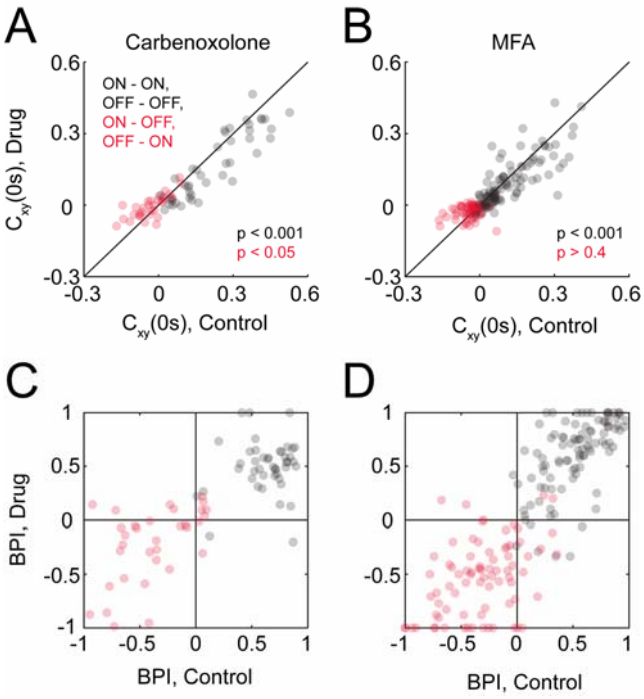

Figure S2. Block of Gap Junctions Reduces Narrow Correlations of Same Sign Cell Pairs but Does Not Change Overall Burst Pattern

(A and B) Each dot represents a pair of cells recorded simultaneously within one recording field at P12 (A: 77 cell pairs, n = 2 retinas; B: 177 cell pairs, n = 2 retinas). Opposite sign cell pairs are shown in red, same sign cell pairs in black. Values along the x-axis indicate the correlation coefficient in a 50 ms time bin around zero time-lag in control conditions. Values along the y-axis represent the same parameter calculated from segments of the recordings during which gap junctions were blocked by 50 μM carbenoxolone (A) or 100 μM meclofenamic acid (MFA) (B) (Pan et al., 2007). Either way of blocking gap junctions reduced these narrow (≤ 50ms) correlations in the spiking of same sign cell pairs, most likely by uncoupling electrical connections between neighboring RGCs and possibly between RGCs and amacrine cells (Brivanlou et al., 1998). As expected, blockade of gap junctions did not consistently change the less than random probability of opposite sign cells to fire together. (C and D) Burst preference for the same cell pairs shown in A and B (black: same sign; red: opposite sign). Burst preference in control conditions is shown along the x-axis. Burst preference in the presence of 50 μM carbenoxolone (C) or 100 μM meclofenamic acid (MFA) (D) along the y-axis. Neither way of blocking gap junctions affected the overall burst pattern of ON and OFF RGCs, arguing that these broader aspects of the cross-correlation function are independent of electrical coupling.

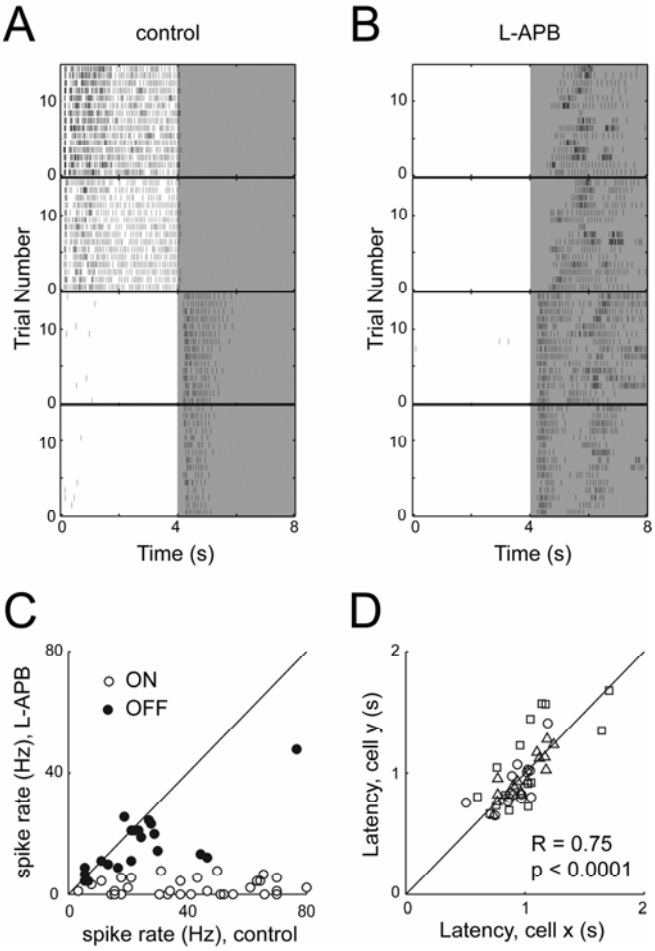

Figure S3. APB Abolishes ON Light Responses at P12

(A and B) Peristimulus rasters of spike trains from simultaneously recorded representative ON (upper two panels) and OFF RGCs (lower two panels) in control conditions (A) or in the presence of 50 μM L-APB (B) during 15 cycles of a full-field stimulus square wave modulated at 0.125 Hz. Shaded areas indicate periods of darkness (~10^1 Rh*/M-cone/s) and unshaded areas indicate periods of illumination (~10^5 Rh*/M-cone/s). (C) Peak spike rate (50 ms time bin) of ON (open circles, 35 cells from 5 retinas) and OFF RGCs (filled circles, 21 cells from 5 retinas) during the respective phase of the stimulus in control conditions (x-axis) and in the presence of 50 μM L-APB (y-axis). Peak spike rate of ON RGCs is reduced to 9.7 ± 2.1% of control while OFF RGC light responses are much less affected (peak spike rate 80 ± 7.1% of control). This reduction of OFF light responses by L-APB might be explained by the presence of L-APB sensitive type III metabotropic glutamate receptors mGluR7 at the axon terminals of OFF cone bipolar cells (Brandstatter et al., 1996) and mGluR8 in both the inner and outer plexiform layer (Koulen and Brandstatter, 2002). As evident in (B) ON cells in the presence of L-APB displayed bursts of activity. These bursts resembled the pattern of spontaneous activity more than light responses in the following aspects. Unlike normal light responses, bursts were not precisely time-locked to the change in stimulus phase, yet in 4 of 5 retinas were restricted to the OFF phase of the stimulus. The timing of this activity appeared synchronized within trials between neighboring cells. (D) Plots of the latency from the offset of light to the first spike during the OFF phase of 15 stimulus trials for three pairs of ON cells in the presence of L-APB. Different cell pairs are indicated by the different symbols. This confirms that there is extensive trial-to-trial variation for onset of firing of ON cells during the OFF phase, while the firing of neighboring cells remains synchronized. OFF RGCs in addition to short latency light responses, displayed similar bursts in the presence of L-APB.

In conclusion, these observations confirm that L-APB effectively blocked all light evoked ON responses in our recordings. In addition, bursts of action potentials that resemble activity patterns observed during waves appear in both ON and OFF RGCs and are clustered in but not precisely timed to the OFF phase of the stimulus. Future experiments are needed to define the mechanisms by which light responses and spontaneous activity interact in the presence of L-APB.

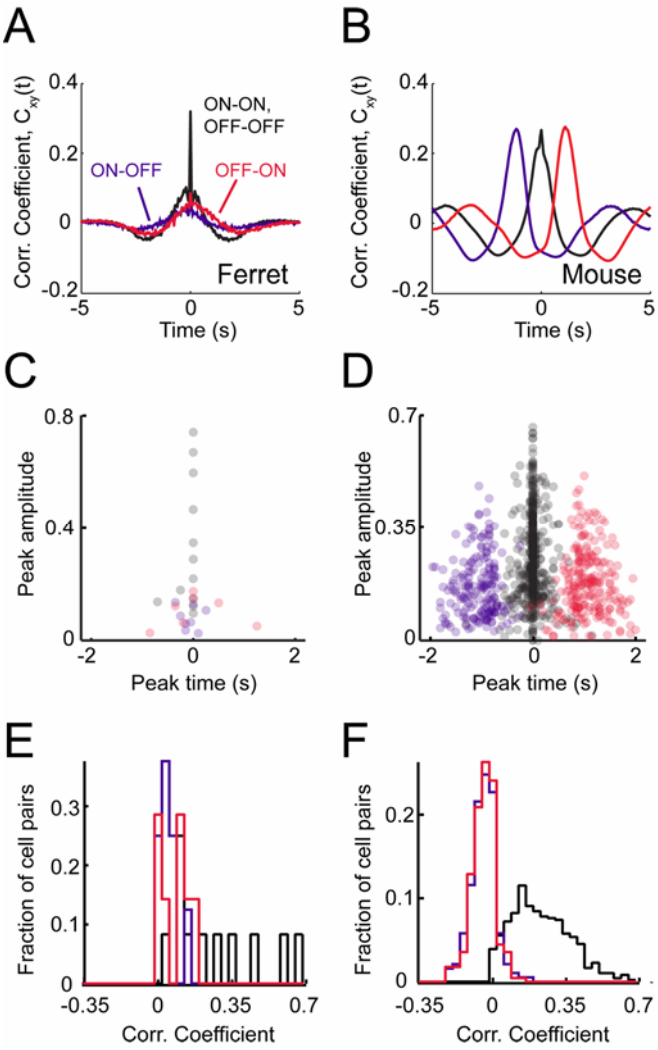

Figure S4. Comparison of Cross-Correlation Structure of ON and OFF RGC Spike Trains during Glutamatergic Waves in Mice and Ferrets

(A and B) Traces represent the average cross-correlations for all ferret RGC pairs presented in (Lee et al., 2002) (A), and for all mouse RGC pairs from one representative experiment of the present study (B). Importantly, in ferrets the temporal structure of the cross-correlograms was very similar for same and opposite sign cell pairs, and to distinguish between them one needs to take into account the amplitude of these traces. By contrast, mouse cross-correlations of same and opposite sign cell pairs have very different temporal structures. (C and D) Dots represents pairs of neighboring RGCs (black: same sign, purple: ON – OFF, red: OFF - ON) recorded simultaneously during glutamatergic waves in ferrets (C, 27 pairs, P16 – P24) and mouse (D, 901 pairs P12) Values along the x-axis indicate peak time of cross-correlation functions. Values along the y-axis represent the value of the cross-correlation at its peak. (E and F) Histograms of the correlation coefficients of the same cell pairs as in (C) and (D). Color coding as before.

Ferret RGCs were recorded using pairs of extracellular electrodes (Lee et al., 2002). At the end of each recording, RGCs were filled with Lucifer yellow and classified as ON or OFF based on their dendritic stratification pattern; the dendritic territories of these cell pairs overlapped. Mouse RGCs were recorded using high density multielectrode arrays and cells were classified as ON or OFF based on their light responses (see Experimental Procedures and Results). Cross-correlations were restricted to cells recorded on electrodes contained within an area smaller than dendritic fields of most RGCs at the ages covered in our study (Diao et al., 2004). Since both studies recorded nearby RGCs with overlapping dendritic territories, we think

that the differences in the cross-correlations of RGC pairs in ferret and mice are likely to reflect species differences (see Discussion), while we concede that it remains possible that future studies sampling a larger number of RGCs in ferrets might still uncover burst patterns similar to those described here for mouse RGCs.

In ferrets neighboring ON and OFF RGCs tend to burst together, whereas in mice they burst in sequence: ON before OFF. We briefly want to relate these differences in activity patterns to the temporal structure of the plasticity rules used in two models of dLGN circuit refinement in ferrets (Butts et al., 2007; Lee et al., 2002). The model with which Lee et al. simulated ON/OFF segregation of retinogeniculate projections used the raw cross-correlation of RGC spike trains at zero time-lag to sample activity patterns of cells. The model with which Butts et al. simulated retinotopic refinement of RGC axons in the dLGN used a BTDP rule. This rule sampled activity correlations approximately over the range of time-lags spanned by cross-correlograms shown in Figure 2. It predicted the strengthening of inputs whose bursts coincided with the bursts of the postsynaptic cell, as well as weakening of inputs that burst shortly before or after it. Importantly, this BTDP rule was experimentally supported (Butts et al., 2007). The similar temporal structure of the activity patterns of same and opposite sign RGCs in ferrets likely means that irrespective of the temporal structure of the plasticity rule used other terms of the model (e.g. competition and inhibition in Lee et al., 2002) need to be relied on heavily to successfully achieve ON/OFF segregation. By contrast, it seems likely that if a rule similar to BTDP were applied to model circuit refinement in the dLGN based on the mouse data presented here, ON/OFF segregation might more stably be instructed by the temporal structure of the RGC activity pattern. It remains possible, however, that future studies of glutamatergic waves in ferrets using MEA recordings might detect similar activity patterns as in mice.